NASA Contractor Report 4588

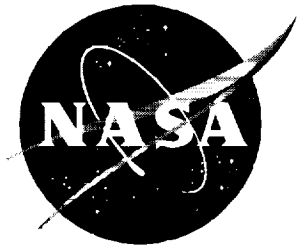

Conceptual Radiometer Design Studies for Earth Observations From Low Earth Orbit

Richard F. Harrington
Old Dominion University • Norfolk, Virginia

National Aeronautics and Space Administration
Langley Research Center • Hampton, Virginia 23681-0001

Prepared for Langley Research Center
under Contract NAS1-18584

April 1994

CONCEPTUAL RADIOMETER DESIGN STUDIES

FOR

EARTH OBSERVATIONS FROM LOW EARTH ORBIT

By

Richard F. Harrington*

ABSTRACT

A conceptual radiometer design study was performed to determine the optimum design approach for spaceborne radiometers in low Earth orbit. Radiometric system configurations which included total power radiometers, unbalanced Dicke radiometers and balanced Dicke or as known as noise injection radiometers were studied. Radiometer receiver configurations which were analyzed included the direct detection radiometer receiver, the double sideband homodyne radiometer receiver and the single sideband heterodyne radiometer receiver.

Radiometer system performance was also studied. This included radiometric sensitivity analysis of the three different radiometer system configurations studied. Both external and internal calibration techniques were analyzed. An accuracy analysis with and without mismatch losses was performed.

It was determined that the balanced Dicke radiometer system configuration with direct detection receivers and external calibrations was optimum where frequent calibration such as once per minute were not feasible.

*Associate Professor of Electrical Engineering Technology, Old Dominion University, Norfolk, Virginia 23529-0243

TABLE OF CONTENTS

INTRODUCTION

The work completed under this task order contract is a part of an overall study sponsored by the Antenna and Microwave Research Branch at the Langley Research Center to develop advanced radiometer technology for geostationary orbit mission applications. Initially the objective of this particular study was to determine the optimum radiometer concepts for use with phased array feed subsystems to achieve wide-scanning of the earth and reflector-distortion compensation during remote sensing operations. This included study efforts to assess radiometer issues of concern in the use of radiometer phased arrays for scanning and reflector compensation to meet the defined sensor mission requirements. These issues included:

(a) Effect of ohmic and mismatch losses within the antenna feed array on radiometric performance.

(b) Effect of low noise amplifiers (LNA's) within the phased array antenna feed network on radiometric sensitivity (ΔT), accuracy and calibration.

(c) Effect of variations in ohmic and mismatch losses within the phased array during scanning or changes in reflector compensation on radiometer system performance.

(d) Radiometric calibration techniques.

(e) Preliminary descriptions of candidate radiometer configurations and their predicted performance.

During the period of performance of this task, significant changes in the overall NASA radiometer development program resulted

in redirection and expansion of the effort under this task. Radiometer design studies for low earth orbit (LEO) missions were emphasized instead of geostationary orbit missions. The emphasis was directed to radiometric remote sensing missions under the NASA Earth Probes Program. This program requires small inexpensive payloads that can be launched from a Pegasus or Taurus launch vehicle. Therefore this research task was expanded to include all types of real aperture antenna radiometer systems.

RADIOMETRIC SYSTEM CONFIGURATIONS

There are three basic radiometer system configurations. These are total power, unbalanced Dicke and balanced Dicke. There are some additional techniques employing automatic gain control (AGC) such as the Hach radiometer and a noise adding radiometer. However, these have not been employed in spacebourne applications. Descriptions of these techniques are readily available[1]. The radiometer receiver employed in each of these radiometric systems can have three types of configurations. These include direct detection, double sideband zero IF homodyne and single sideband heterodyne. The selection of which of the nine possible combination of configurations is based on the required radiometer performance.

The radiometric system performance requirements which effect the choice of configurations include:

(1) Radiometric sensitivity

(2) Calibration techniques

(3) Linearity

(4) Accuracy

(5) Losses and mismatches

(6) Dynamic range

(7) Primary power requirements

(8) Weight

The effect of the various radiometer configurations on the performance requirements will be discussed during the description of each type of configuration.

Total Power

The total power radiometer system configuration is illustrated in Figure 1. This configuration consists of a radiometer receiver which is connected directly to the antenna. The electromagnetic radiation received by the antenna is defined as the **antenna radiometric temperature, T_A** [1]. The antenna radiometric temperature is related to the power received, P, using the Rayleigh-Jeans approximation of Planck's radiation law[1]:

$$P = kT_AB \quad \text{W} \tag{1}$$

where:

k = Boltzmann's constant = 1.38×10^{-23} joule K^{-1}

B = Bandwidth, Hz

The radiometer receiver generates noise internally. The commonly accepted practice is to relate this internally generated receiver noise to a noise generator at the input of a noise-free receiver. This noise generator will produce the same noise power output as the internally generated noise. The output noise power of this input noise generator is defined as the **effective input noise temperature, T_{RAD}**. The actual noise power can be determined from (1) by substituting T_{RAD} for T_A. The incoming antenna radiometric temperature noise signal has similar characteristics as the receiver noise. These two noise signals are added together in the receiver and can not be separated. Therefore the effective input signal to the noise-free radiometer receiver is a Gaussian noise signal with zero mean and a variance equal to the total noise power. The input can be represented by

$$T_{sys} = T_A + T_{RAD} \quad (2)$$

where:

T_{sys} = system temperature, K

T_A = antenna radiometric temperature, K

T_{RAD} = effective input noise temperature, K

The noise-free receiver has a gain G and a bandwidth B. The output of the receiver is the input to a square law detector whose output voltage is proportional to the input power. The square law detector power sensitivity constant C_d determines the output voltage as a function of the input power, i.e. volts per watt. The output of the square law detector is a noisy dc voltage which is smoothed by the low pass filter. The low pass filter has an equivalent integration time τ. The output voltage V_{out} is:

$$V_{out} = k(T_A + T_{RAD})BGC_d \quad (3)$$

Instabilities in the effective input noise temperature T_{RAD} and the overall gain G of the radiometer will create random variations in V_{out}. This additional noise limits the radiometric sensitivity of the total power radiometer configuration.

Unbalanced Dicke

The unbalanced Dicke radiometer system configuration is illustrated in Figure 2. This configuration was developed by R. H. Dicke to eliminate the effects of 1/f noise in the measurement of noisy signals. An amplifier has two basic noise sources. One is a gaussian white noise which has the same noise power spectral

density at all frequencies within the bandwidth of the amplifier while the other has a noise power spectral density which increases with decreasing frequency within the bandwidth of the amplifier. The desired output signal from a total power radiometer is a dc voltage. The noisy variations of this dc voltage is reduced by reducing the noise bandwidth of the radiometer. This is accomplished integrating the output of the square law detector. If the noise is uniform white noise, then the total noise power is reduced as the bandwidth is reduced. However, if the noise power spectral density has a 1/f characteristic, the noise power is constant with decreasing noise bandwidth and no improvement in signal to noise ratio is achieved by integration of the output signal.

Dicke observed this problem while attempting to measure low level dc voltages associated with antenna measurements during World War II. There is a frequency within the bandwidth of the amplifier where the white noise is greater than the 1/f noise. At any frequencies above this frequency, a measurement of a desired signal could be achieved and the signal to noise ratio improved by reducing the noise bandwidth of the measurement through integration.

Dicke achieved this by periodically switching the input of the amplifier between the antenna and a reference load. Referring to Fig 2., the input to the radiometer receiver during the time that the input switch is connected to the antenna is a noise power proportional to $T_A + T_{RAD}$. During the time the input switch is

connected to the reference load, the input to the radiometer receiver is a noise power proportional to $T_{REF} + T_{RAD}$ where T_{REF} is the physical temperature of the reference load. This varying power signal is converted within the square law detector to voltage square wave with a peak to peak amplitude proportional to $T_{REF} - T_A$. The fundamental frequency of this square wave is above the frequency where the 1/f noise has any effect. This signal is synchronously detected which results in a dc voltage proportional to $T_{REF} - T_A$ which can be integrated to improve the signal to noise ratio. Thee voltage output the unbalanced Dicke radiometer is:

$$V_{out} = k\,(T_{REF} - T_A)\,BGC_d \qquad \textbf{(4)}$$

Comparison of (3) and (4) shows that the variations in the internal noise T_{RAD} of the radiometer does not effect the output voltage of the unbalanced Dicke radiometer as it does to the total power radiometer. However gain variations within the radiometer receiver still has an effect on the output voltage.

The disadvantage of the unbalanced Dicke is that the radiometer is performing a measurement only 50% of the time as that of the total power radiometer. Therefore the allowable integration time is half that of the total power radiometer. It will be shown later that this decreases the sensitivity of the unbalanced radiometer.

The variations in the output voltage due to gain variations could be eliminated if the power level into the radiometer receiver while the switch is connected to the antenna could be made identical to the power level when the switch is connected to the

reference load. This configuration is referred to as a balanced Dicke radiometer system configuration.

Balanced Dicke

The balanced Dicke radiometer system configuration is illustrated in Figure 3. A summing network, typically a directional coupler, is inserted between the antenna and the switch which switches between the antenna and the reference load. This switch is commonly referred to as the Dicke switch. Noise is added to the antenna noise, the antenna radiometric temperature T_A. This noise is defined as the injected noise T_{inj}. The sum of the antenna radiometric temperature and the injected noise temperature is made equal to the Dicke reference temperature.

$$T_A + T_{INJ} = T_{REF} \tag{5}$$

A closed loop feedback system continuously adjusts the amount of the injection noise such that the output of the synchronous detector is maintained at a null or zero. Therefore the variations both in the internal noise within the radiometer receiver and variations in the gain of the radiometer receiver are eliminated from the output of the radiometer. The magnitude of the signal which controls the amplitude of the injected noise is a measure of the antenna radiometric temperature through the use of (5) above.

The disadvantage of the balanced Dicke radiometer is that the system temperature T_{SYS} is greater for the balanced Dicke over the unbalanced Dicke. However, the effects of gain variations in the unbalanced usually have a larger degradation of sensitivity than

the higher system temperature.

The balanced Dicke radiometer system configuration is also referred to a noise injection radiometer in some references. The method to control the injected noise level is to use a noise injection switch. The avalanche noise diode is operated continuously for stability. Two methods have been proposed. The noise injection can be achieved by narrow fixed width pulses where the number of pulses is varied. The other method is to use one pulse where the pulse width is varied.

RADIOMETER RECEIVER CONFIGURATIONS

There are three basic radiometer receiver configurations which can be used to implement any of the three radiometer system configurations discussed above. These include direct detection, double sideband homodyne and single sideband heterodyne.

Direct Detection

The direct detection receiver configuration is illustrated in Figure 4. All amplification, prior to the square law detector, of the desired noise bandwidth is accomplished at the rf frequency of interest. Therefore the input to the square law detector is at the rf frequency. Recent advances in technology has allowed the development of square law detectors up to 100 GHz. The critical specifications are linearity output voltage as a function of input power and good sensitivity.

The first component is a low noise amplifier (LNA) which must be located as close to the antenna feed as possible to minimize front end losses. After some amplification, a RF filter is used to select the desired bandwidth at the desired operating frequency. Typical gain for the LNA is 25 to 30 dB. Additional RF gain is needed after the RF filter to achieve a system gain of approximately 55 to 60 dB gain prior to the square law detector. The sensitivity of most square law detectors is approximately -25 dBm. The output of the square law detector is video amplified and either low pass filtered or integrated to achieve the required radiometric sensitivity.

The advantage of direct detection is low dc power requirements, less weight and volume due to fewer components and less susceptible to radio frequency interference (RFI). Direct detection receiver configurations are being used up to 37 GHz in the Special Sensor Microwave Imager Sounder (SSMIS). The SSMIS is being developed by Aerojet for use on future Defense Meteorological Satellite Program (DMSP) satellites. The Tropical Rainfall Mapping Mission (TRMM) Microwave Imager (TMI) being developed by Hughes Aircraft Co. for NASA-Goddard will use direct detection up to 37 GHz and are looking at using direct detection at 85.5 GHz.

Direct detection radiometer receiver configuration will be the choice for all types of radiometer system configurations up to RF frequencies of 37 GHz. The direct detection receiver also might be used up to 100 GHz. Therefore applied research into the stability of the gain and internally generated noise in low noise amplifiers is essential to the improvement of microwave radiometer technology for future spaceborne applications.

Double Sideband Homodyne Receiver

The double sideband homodyne receiver configuration is illustrated in Figure 5. The desired measurement frequency band is centered at the RF frequency of interest. The first component in the receiver configuration is a RF mixer-IF preamplifier combination. A local oscillator (LO) is used to frequency translate the desired frequency band, centered about a RF frequency which is equal to the LO frequency, down to a baseband frequency.

The RF mixer multiplies the RF frequency band by LO frequency which produces both the sum and difference frequencies. The IF preamplifier selects the difference frequencies, which occupy a band from dc to B/2. B is the bandwidth of the RF measurement frequency band. The local oscillator produces noise which would interfere with the measurement. Therefore this noise is eliminated by the IF bandpass filter whose bandwidth is from typically 1 MHz to B/2. The input to the square law detector is at the IF baseband frequencies where good linearity and sensitivity is easily accomplished.

This receiver configuration was widely used in many radiometric applications in the past. Prior to the development of good microwave low noise amplifiers, this configuration offered the lowest effective input receiver noise temperature. The low noise aspect of this configuration resulted from the requirement that the noise being measured by the radiometer is white gaussian noise and has a constant noise power spectral density over the entire bandwidth of interest, B. The internally generated noise in the IF preamplifier is only over a bandwidth of B/2 - 1 MHz. Therefore there is twice the noise power to be measured as the noise power causing interference to the measurement. Mixer manufacturers specified the noise figure of mixers used in this radiometer receiver configuration as "double sideband noise figure". This is typically 3 dB better than the actual noise figure of the mixer.

This configuration was employed in the past in the NASA-Goddard and JPL Scanning Multifrequency Microwave Radiometer (SMMR)

flown on Nimbus-7 and Seasat respectfully. The configuration is also used in the Special Sensor Microwave/Imager (SSM/I) presently being flown on the DMSP satellites. The SMMR's are unbalanced Dicke radiometer system configuration while the SSM/I is a total power radiometer system configuration. The SSM/I was the first spaceborne application to employ the total power configuration. Previous spaceborne radiometers where almost always utilized the unbalanced Dicke configuration.

The double sideband homodyne receiver configuration will be used at frequencies where low noise amplifiers and direct detection square law detectors are not available. Radiometer receivers operating above 100 GHz will be using this configuration in the future.

Single Sideband Heterodyne Receiver

The single sideband heterodyne receiver configuration is illustrated in Figure 6. This configuration uses a low noise amplifier prior to the mixer preamplifier. The LNA establishes the noise figure of the radiometer receiver. One of the sidebands is rejected by the sideband rejection filter prior to the mixing process by the mixer and LO. Therefore the IF frequency band does not have to be near dc, but can be at any frequency where a good square law detector is available. The IF bandpass filter establishes the desired RF measurement bandwidth B over which the measurement is made. This configuration is used where LNA's are available but square law detectors are not.

The principal application of this receiver configuration is in temperature sounding applications in the 50 to 60 GHz oxygen absorption band. SSMIS temperature sounding channels will use this configuration. Also the future Advanced Microwave Sounding Units (AMSU) will employ this configuration.

RADIOMETER SYSTEM PERFORMANCE REQUIREMENTS

Several of the radiometer system performance requirements which effect the design of a spaceborne radiometer system will be discussed in detail. These include radiometric sensitivity, calibration techniques, effect of front-end losses, effect of mismatches, and accuracy.

RADIOMETRIC SENSITIVITY

The radiometer sensitivity (resolution) is the minimum change in the radiometric antenna temperature that can be detected in the radiometer output. This is defined as a change in the output equal to the standard deviation of the output. The input to a radiometer is a gaussian random noise signal. An ideal total power radiometer with no gain fluctuations would have a resolution given by [1]:

$$\Delta T_{IDEAL} = \frac{T_{SYS}}{\sqrt{B\tau}} \qquad (6)$$

where $T_{SYS} = T_A + T_{REC}$

T_A = Radiometric antenna temperature

T_{REC} = Receiver input noise temperature

T_{SYS} = Radiometer system temperature

B = Predetection bandwidth

τ = Postdetection integration time

The radiometer amplifies the noise due to the radiometric antenna temperature and receiver input noise temperature by a large

gain to produce a useable output signal. There are random fluctuations in the radiometer output due to thermal and non-thermal induced random fluctuations in the overall radiometer receiver gain. The effects of gain fluctuations are root-sum-squared with the ideal radiometer fluctuation. The sensitivity equation is given by [1]:

$$\Delta T_A = T_{SYS}\left[\frac{1}{B\tau} + \left(\frac{\Delta G_s}{G_s}\right)^2\right]^{1/2} \qquad (7)$$

where ΔT_A = radiometric antenna temperature sensitivity.

G_S = average system power gain.

ΔG_S = effective value (RMS) of gain variations.

Other error sources, which produce fluctuation in the radiometer output can be added (root sum squared) to (7) above. Examples of these include quantization noise in radiometer with digitized output and noise introduced after detection by the video amplifier stages in the radiometer receiver. These errors sources should be made insignificant through proper design techniques.

The sensitivity of the radiometric brightness temperature (ΔT_B) measurement will be worse than the sensitivity of the radiometric antenna temperature measurement (ΔT_A). The equation for radiometric brightness temperature sensitivity is:

$$\Delta T_B = K_{apc}\,\Delta T_A \qquad (8)$$

where K_{apc} is a scale factor determined by the antenna pattern correction algorithm. The value of K_{apc} will depend on the number of measurements involved in the antenna pattern correction

algorithm and the degree of decorrelation between these measurements.

The sensitivity of a unbalanced Dicke radiometer is given by [1]:

$$\Delta T_A = \left[\frac{2(T_A + T_{REC})^2}{B\tau} + \frac{2(T_{REF} + T_{REC})^2}{B\tau} + \left(\frac{\Delta G_s}{\Delta G_s}\right)^2 (T_A - T_{REF})^2 \right]^{1/2} \quad (9)$$

where T_{REF} is the physical temperature of the reference matched load. Comparison of equation (9) with equation (7) for the total power radiometer shows that the effect of gain fluctuations have been reduced by the factor:

$$\left[\frac{(T_A + T_{REC})}{(T_A - T_{REF})} \right]^{1/2} \quad (10)$$

The effects of gain fluctuations can be eliminated in equation (9) if T_A is made equal to T_{REF} by adding injected noise in the antenna input to the radiometric antenna temperature noise. This is the balanced Dicke radiometer or more commonly referred to as the noise injection radiometer (NIR). The radiometric antenna temperature sensitivity equation for a balanced noise-injection Dicke radiometer is obtained from equation (9) by letting $T_A = T_{REF}$:

$$\Delta T_A = \frac{2(T_{REF} + T_{REC})}{\sqrt{B\tau}} \quad (11)$$

ACCURACY

The overall accuracy of the radiometric brightness temperature measurements is affected by various error sources. The most significant error sources include:

(a) Radiometric sensitivity, ΔT_a, of the measurement of the scene antenna temperature.

(b) Radiometric sensitivity, ΔT_h and ΔT_c, of the measurement of the hot load calibration temperature and the cold sky antenna calibration measurement.

(c) Effect of thermal and non-thermal induced gain fluctuations on the ΔT_a, ΔT_h and ΔT_c radiometric sensitivities during the measurement of T_a, T_h, and T_c.

(d) Effect of dissipative and mismatch losses on the correction algorithms to determine the radiometric antenna temperature, hot load radiometric temperature and cold sky radiometric temperature.

(e) Uncertainties in measurement of reflection coefficients, attenuations, physical temperatures and estimation of the cold sky radiometric antenna. The uncertainties in these measurements produce an uncertainty in the correction algorithms used to determine T_A, T_h, and T_c.

(f) Effect of the antenna pattern correction algorithm used to determine the scene radiometric brightness temperature from the scene radiometric antenna temperature measurement. This effect will increase the overall standard deviation of the radiometric brightness temperature measurement.

Errors Due To Gain Fluctuations

Thermal and non-thermal induced gain fluctuations produce errors in both total power and Dicke radiometers. The magnitude of non-thermal induced gain fluctuations for a total power radiometer have been analytically and experimentally determined by Hersman and Poe [2]. The gain fluctuation, $\Delta G/G$, is a function of the integration time during measurement, integration time during calibration, time between calibration, the calibration estimator weighing function, and the receiver output fluctuation power spectral density [$S_g(f)$]. The receiver output fluctuation power spectral density consists of two components; a uniform power spectral density [$S_i(f)$] and a $1/f^{\alpha}$ power spectral density [$S_g(f)$] which decreases with frequency. A value determined experimentally by Hersman and Poe[2] for a total power radiometer without a low noise RF amplifier (LNA) is

$$S_g(f) = \frac{(1.3 \times 10^{-10})}{f^{1.3}} \qquad H_z^{-1}(normalized) \qquad (7)$$

The uniform component is:

$$S_i(f) = 1.5 \times 10^{-9} \qquad H_z^{-1}\ (normalized) \qquad (8)$$

The value of $S_g(f)$ was used to determined $(\Delta G/G)^2$ for the condition where calibration integration time is ten times longer than the scene integration time. The scene integration time was set to 1 millisecond and a correction factor determined for longer scene integration times. This data is presented in Figure 12 of Hersman and Poe's paper. Using this data, the value of $(\Delta G/G)^2$ for a scene integration time for 1 second, a hot and cold integration time of 10 seconds and a calibration period T_c, that is varied from 10 seconds to 10,000 seconds was computed. Table 1 below gives the

value of $\left(\frac{\Delta G}{G}\right)^2$ as a function of time between calibrations

TABLE 1	
T_c (seconds)	$(\Delta G/G)^2$
10	1×10^{-9}
100	5×10^{-9}
1000	1×10^{-8}
10000	2×10^{-8}

These values are believed to be typical for the non-thermal induced gain fluctuations. Thermal induced gain fluctuation for low noise millimeter wave amplifiers are typically 0.015 dB per °C stage [3]. A typical gain per stage is 7 dB; therefore, the $\left(\frac{\Delta G}{G}\right)$ per stage is 3.46×10^{-3} per °C. Using temperature compensation techniques, total power radiometers have achieved a thermal induced gain variation of 0.05 dB per °C or 0.012 per °C. The total gain fluctuation, $\left(\frac{\Delta G}{G}\right)_t$ is the sum of the $\frac{\Delta G}{G}$ of each stage if $\frac{\Delta G}{G} \ll 1$ and n = number of stages.

$$\left(\frac{\Delta G}{G}\right)_t = \sum_{i=1}^{n} \left(\frac{\Delta G}{G}\right)_i \qquad (9)$$

Assuming 5 stages of low noise amplitude prior to the mixer-preamplifier, the total $\left(\frac{\Delta G}{G}\right)_t$ for the video amplifiers, DC amplifiers and RF input circuit components can be estimated to be of the same order as the low noise amplifier resulting in a overall $\left(\frac{\Delta G}{G}\right)$ for the total power radiometer of 1.7×10^{-2} per °C. The thermal induced gain variation of 0.015 per °C will be used in this

analysis. An additional source of gain fluctuation are those produced by power supply voltage fluctuations. It is assumed that the voltage regulation of the power supply employed in the total power radiometer can be designed to maintain the gain fluctuations due to voltage fluctuations an order of magnitude below the other sources of gain fluctuations. However, if a total power radiometer is chosen, a through analysis of this source of gain fluctuations must be undertaken in order to properly determine specifications for the power supply design.

The three sources of gain fluctuations, non-thermal due to $1/f$ receiver noise, thermally-induced and voltage induced are statistically independent random noise errors. The overall gain fluctuations is the root sum square of these three sources.

An estimate of the thermal stability requirement for the total power radiometer can be determined by allowing the radiometric sensitivity of the total power radiometer to equal the radiometric sensitivity of the balanced noise-injection Dicke radiometer. The radiometer sensitivity of the noise-injection radiometer (NIR) can be determined from equation (6) with T_{REF} equal to 298 K and T_{REC} equal to 676 K. The bandwidth is 200 MHz and integration time of 1 seconds. The NIR radiometric sensitivity is therefore 0.14 K. The allowable $\left(\frac{\Delta G}{G}\right)_o$ for the total power radiometer (TPR) can be

determined from equation (2) with T_{SYS} equal to T_A of 298 K plus T_{REC} of 676 K or 974 K. The bandwidth is 200 MHz and the integration time is 750 millisecond. The allowable ΔT_A is 0.14 K, then the same as the NIR design.

Therefore, the allowable $\left(\frac{\Delta G}{G}\right)_t$ is

$$\left(\frac{\Delta G}{G}\right)_o = \sqrt{\left(\frac{\Delta T_A}{T_{syst}}\right)^2 - \frac{1}{B\tau}} \qquad (10)$$

After substitution of values stated above, the allowable $\left(\frac{\Delta G}{G}\right)_o$ is

1.18×10^{-4}.

The non-thermal induced gain fluctuations is determined by the time between calibrations using data from Table 1. Using the external calibration scheme with the scene being measured for 750 milliseconds, the hot load for 100 milliseconds and the cold load for 100 milliseconds every second and requiring that the integration times of the hot and cold temperature calibrations be hundred times that of the scene temperature integration time results in a period between calibrations of 75 seconds. This will reduce the fluctuations in the hot and cold calibrations to one tenth of the fluctuations in the scene measurement. The non-thermal fluctuations for a 75 second time between calibrations is 3.01×10^{-5} as interpolated from Table 1. The allowable thermally induced gain fluctuations can be attained from the following equation:

$$\left(\frac{\Delta G}{G}\right)_t = \left[\left(\frac{\Delta G}{G}\right)_o^2 - \left(\frac{\Delta G}{G}\right)_{nt}^2\right]^{1/2} \quad (11)$$

where $\left(\frac{\Delta G}{G}\right)_o$ = *overall allowable* $\frac{\Delta G}{G}$

$\left(\frac{\Delta G}{G}\right)_{nt}$ = *non-thermal* $\frac{\Delta G}{G}$

$\left(\frac{\Delta G}{G}\right)_t$ = *thermally induced* $\frac{\Delta G}{G}$

Note: *It is assumed that the voltage induced* $\left(\frac{\Delta G}{G}\right)$ *is less than* 1/10

Using the equation above, the thermally-induced gain fluctuations must be less than 1.14×10^{-4}.

The estimated thermally-induced gain fluctuations for the radiometer is 1.5×10^{-2} per °C. Since the maximum allowable thermally-induced gain fluctuations is 1.14×10^{-4}, then the maximum allowable temperature variations during the calibration period is 7.61×10^{-3} °C. The calibration period is 75 seconds resulting in a thermal stability requirement for the total power radiometer including the RF input section, low noise amplifier and the mixer preamplifier is 1.01×10^{-4} °C per second or 0.36 °C per hour.

The thermal stability requirement for the low frequency signal processor portion of a total power radiometer was determined experimentally by Neils Skou of the Technical University of Denmark[4]. The radiometric temperature varied 5 K for a 12 °C change in physical temperature of the low frequency signal processor portion of the total power radiometer. The radiometric temperature output of the noise-injection radiometer did not vary during the same 12°C change in physical temperature due to the

closed-loop feedback design inherent in a noise-injection radiometer.

The temperature stability of the signal processor portion should be capable of maintaining less than a 0.1 K error during the calibration period. This results in a temperature stability requirement of 0.02° per minute or 1.2°C per hour for the low frequency signal processor portion of a total power radiometer. Experience with the low-frequency signal processor portions of noise-injection radiometers showed no error due to temperature variations. The Stepped Frequency Microwave Radiometer (SFMR)[5] and Pushbroom Microwave Radiometer (PBMR)[6] did not have any temperature control on the signal processor portions. There was no detectable errors due to the lack of thermal control.

The thermal stability requirement for the RF portion, low noise amplifiers and mixer-preamplifier portion of a noise-injection radiometer is 0.1 °C. over any time period. This was achieved in both the SFMR[5] and the PBMR[6]. Temperature stabilities much worse than 0.1 °C can be tolerated in noise-injection radiometers by simple temperature correction algorithms. Experiments on a noise injection radiometer by Skou[4] demonstrated that the error in the radiometric antenna temperature was $\pm$ 0.2 K while the RF portion, low noise amplifier and mixer-preamplifier was subjected to temperature variations from -25 °C to +20 °C using a simple linear temperature correction algorithm.

In summary, the temperature stability requirements for a total power radiometer are very stringent in order to have a radiometric sensitivity equal to that of a noise-injection radiometer. The temperature stability requirements of a noise injection radiometer easily can be achieved.

Error Analysis Without Mismatch Loss

An error analysis computer program based on a radiometric antenna temperature measurement with a hot load and cold sky calibrations using the Y-factor method was obtained from Brett Pigon of the Harris Corporation, Melbourne, FL. This program did not include the effects of mismatch loss and the uncertainties associated with the reflection coefficient measurements. The effects of mismatch loss is discussed in the next section.

The error analysis program was used to determine the error in the radiometric antenna temperature measurement with the radiometer. Four different cases were analyzed. These included:

Case 1: A radiometer in which the sensitivities of the scene measurement, ΔT_A; the hot load measurement, ΔT_H; and the cold sky calibration measurement, ΔT_c are equal. An internal calibration technique was employed.

Case 2: The sensitivities of the hot load, ΔT_H, and cold sky ΔT_C were made to be 1/10 of the scene measurement, ΔT_A. Internal calibration was used.

Case 3: The sensitivities are the same as case 1, however an external calibration scheme was employed.

Case 4: The sensitivities are the same as case 2, however an external calibration scheme was employed.

The internal calibration technique is one in which a switch is used to switch from the scene antenna to either the hot load or the cold-sky antenna. The hot-load, calibration switches, and the radiometer RF components are located in a constant temperature

enclosure. The scene antenna and the waveguide from the constant temperature enclosure to the antenna are at a different temperature that is not controlled. The cold-sky antenna and feed waveguide are also outside the constant temperature. Therefore there are three different paths from the scene antenna, the cold-sky antenna, and the hot-load to the input of the radiometer receiver. The dissipative losses, reflection coefficients and physical temperatures of each path must be accurately known in order to correct for their affects on the calibration of the radiometer. The error analysis includes the dissipative loss uncertainties and physical temperature measurement uncertainties, but not those associated with the mismatch loss.

The results of the internal calibration techniques can be seen by examining Case I shown in Table 3 and Case 2 shown in Table 4. Table 2 provide the assumed uncertainties in the hot-load physical temperature (σT_H), the cold-sky radiometric temperature (σT_c), the constant temperature enclosure (σT_2), the physical temperature of the scene antenna waveguide (σT_1), the physical temperature of the cold-sky antenna waveguide (σT_4), and the dissipative losses (σ_L)).

The external calibration techniques employs a common feed horn and a reflection plate which is external to the feed horn. The reflection plate is rotated such that the feed horn views the scene antenna reflector, the hot-load or the cold-sky. The feed horn can be located in the constant temperature enclosure. Therefore the dissipative losses and the reflection coefficients are common to all three paths. The only variable is the reflection coefficient of the feed horn as it views the three different targets, i.e. the scene antenna reflector, the hot-load and the cold-sky.

Table 3, 4, 5 and 6 present the results of the error analysis without mismatch loss or mismatch loss uncertainties for cases 1, 2, 3, and 4 respectfully. The errors are presented as worst case errors which assumes all error sources are correlated and as root sum square which assumes all error sources are uncorrelated. The actual case is closer to the root sum square case, however, there might be some correlation which would increase slightly the actual error.

TABLE 2 - ERROR ANALYSIS UNCERTAINTIES	
Cold Sky Radiometric Temperature (σT_C)	0.2 K
Hot Load Physical Temperature (σT_H)	0.1 K
Constant Temperature Enclosure (σT_2)	0.1 K
Cold Sky Waveguide Physical Temperature (σT_4)	1.0 K
Antenna Waveguide Physical Temperature (σT_1)	1.0 K
Dissipative Losses (σL_{ij})	.012
Radiometric Sensitivity, T_{1N} = 100 K (ΔT_A)	.18 K
Radiometric Sensitivity, T_{1N} = 200 K (ΔT_A)	.20 K
Radiometric Sensitivity, T_{1N} = 300 K (ΔT_A)	.22 K

TABLE 3 - ERROR ANALYSIS FOR CASE 1		
$\Delta T_A = \Delta T_H = \Delta T_C$	Internal Calibration	
T_{1N}	Worst Case Error	Root Sum Square
100 K	8.45 K	4.20 K
200 K	5.12 K	2.32 K
300 K	2.41 K	0.98 K

TABLE 4 - ERROR ANALYSIS FOR CASE 2		
ΔT_H = 1/10 ΔT_A	Internal Calibration	ΔT_C = 1/10 ΔT_A
T_{IN}	Worst Case Error	Root Sum Square
100 K	8.01 K	4.17 K
200 K	4.44 K	2.25 K
300 K	1.50 K	0.64 K

TABLE 5 - ERROR ANALYSIS FOR CASE 3		
	ΔT_A = ΔT_H = ΔT_C Calibration	External
T_{IN}	Worst Case Error	Root Sum Square
100 K	0.82 K	0.52 K
200 K	0.88 K	0.60 K
300 K	0.98 K	0.70 K

TABLE 6 - ERROR ANALYSIS FOR CASE 4		
ΔT_H = 1/10 ΔT_A	External Calibration	ΔT_C = 1/10 ΔT_A
T_{IN}	Worst Case Error	Root Sum Square
100 K	0.39 K	0.21 K
200 K	0.36 K	0.19 K
300 K	0.37 K	0.21 K

Examination of the results in Table 3 thru 6 shows a significant difference between the internal calibration technique and external calibration.

Errors Due To Mismatch Loss

A detailed analysis of the effects of mismatch loss on the absolute noise-temperature calibration of principal noise sources in a microwave receiving system was performed by Tom Y. Otoshi of the Jet Propulsion Laboratory at the California Institute of Technology[7]. Otoshi utilized the Y factor method with a hot and cold load calibrations. This analysis formed the basis for the computer program to predict the range of errors due to mismatch loss.

This program was used to determine the range of mismatch losses for various radiometric antenna temperature from 100 K to 300 K. All possible combinations of five reflections coefficients, each assumed to be positive and negative were used to calculate the 32 possible combinations of phases of the reflection coefficients. The mean and standard deviation of the 32 possible combinations along with the maximum positive error and maximum negative error are presented in Table 7. The hot-load calibration temperature was 298 K and the cold sky calibration temperature was 3 K. The losses and reflection coefficients used in this analysis are listed in Table 8 and Table 9.

TABLE 7 MISMATCH LOSS ERRORS

Antenna Temperature	100 K	200 K	300 K
Mean	97.26 K	198.50 K	300.19 K
Standard Deviation	5.01 K	6.59 K	9.17 K
Bias Error	-2.74 K	-1.50 K	+0.19 K
Maximum Positive Error	+7.23 K	+8.89 K	+12.51 K
Maximum Negative Error	-12.69 K	-12.91 K	-13.13 K

TABLE 8 - DISSIPATIVE POWER LOSS RATIO (dB)	
Hot Load To Receiver Input (L_{GC})	0.5 dB
Cold-Sky Antenna To Calibration Switch (L_{EF})	0.5 dB
Calibration Switch (Cold) to Receiver Input (L_{CE})	0.5 dB
Scene Antenna To Antenna Switch (L_{AB})	0.57 dB
Antenna Switch To Receiver Input (L_{BC})	0.33 dB

TABLE 9 - REFLECTION COEFFICIENT	
Hot Load Output (Γ_H)	.056
Input Of Network I Between Hot Load And Receiver (I_{11})	.048
Output Of Network I (Γ_{2I})	$\pm$.052
Cold Sky Horn and Waveguide Output (Γ_C)	$\pm$.056
Input Of Network D Between Cold Sky Horn And Receiver (D_{11})	.056
Output Of Network D (Γ_{2D})	$\pm$.056
Antenna And Waveguide Output (Γ_A)	$\pm$.126
Input Of Network B Between Antenna And Receiver (B_{11})	.048
Output Of Network B (Γ_{2B})	$\pm$.078
Input Of Receiver (Γ_{1R})	.0126

Note: The five reflections coefficients with $\pm$ before the value are those whose sign makes a difference in the measured radiometric antenna temperature estimation. I_{11}, D_{11}, and B_{11} are used in combinations with Γ_{2I}, Γ_C, Γ_A, Γ_{2B} and Γ_{2D} therefore result in no new combinations. Since the hot load is in the same constant temperature enclosure as the losses and microwave receiver, there is no error in T_H and therefore the sign of Γ_H has no significance.

The mismatch loss errors listed in Table 7 are significant and exceed the error specification of 0.7 K. However, if these are

fixed bias error, they can be removed during calibration by using measurements of the physical temperatures, dissipative power loss and reflection coefficients and computer algorithms to correct for the mismatch loss error. The uncertainties in the physical temperature, dissipative power loss and reflection coefficients and their variations with temperature will result in a random bias error which contributes to the standard deviation of the radiometric antenna temperature measurement.

Mismatch loss errors are not affected by the choice of a total power radiometer or a balanced noise-injection Dicke radiometer. They are significantly reduced by using an external calibration technique versus the internal calibration technique. Although an analysis of mismatch error for an external calibration technique has not been performed, it is apparent that if the same antenna and feed network between the antenna and receiver is used to measure the scene, the cold sky and the hot load, the effects of mismatch are significantly reduced.

SUMMARY AND CONCLUSIONS

A conceptual radiometer design study was performed to determine the optimum design approach for spaceborne radiometers in low Earth orbit. Radiometric system configurations which included total power radiometers, unbalanced Dicke radiometers and balanced Dicke or as known as noise injection radiometers were studied. Radiometer receiver configurations which were analyzed included the direct detection radiometer receiver, the double sideband homodyne radiometer receiver and the single sideband heterodyne radiometer receiver.

Radiometer system performance was also studied. This included radiometric sensitivity analysis of the three different radiometer system configurations studied. Both external and internal calibration techniques were analyzed. An accuracy analysis with and without mismatch losses was performed.

This study showed that for spaceborne application where external calibrations could be performed fairly often, typically less than every minute, the total power radiometer was superior. For applications where external calibrations could not be performed in less than every minute or two, then the balanced Dicke or noise injection radiometer is superior. However, due to a lack of data on gain stabilities of radiometer components and noise diode calibration sources, these conclusions can not be substantiated. Therefore it is recommended that a precision radiometer research laboratory be developed to investigate the stability of low noise amplifiers, radiometer passive components and avalanche noise diodes.

The direct detection radiometer receiver configuration should

be used for all frequencies where low noise amplifiers and square law detectors are available. At the present time, this is up to 50 GHz and in some cases 100 GHz. At frequencies where square law detectors are not capable of meeting the linearity requirements, then the single sideband heterodyne radiometer receiver configuration should be employed. The double sideband homodyne radiometer receiver configuration should only be used at frequencies where low noise amplifiers are not available.

REFERENCES

[1] F.T. Ulaby, R.K. Moore, and A. K. Fung; Microwave Remote Sensing - Active and Passive, Volume 1 Fundamentals and Radiometry; Addison-Wesley, Reading MA, 1981.

[2] Hersman, M. S. and Poe, Gene A.: "Sensitivity of the Total Power Radiometer with Periodic Absolute Calibration." *IEEE Transactions on Microwave Theory and Techniques*, Vol MTT-29, No. 1, pp 32-40, January 1981.

[3] MITEQ, MITEQ Amplifier Handbook Miteq, Hauppauge, NY; 1986.

[4] Skou, N. Microwave Radiometer Systems: Design and Analysis. Aertech House, Inc. Norwood MA; 1989.

[5] Harrington, R. F.: "The Development of a Stepped Frequency Radiometer and its Application to Remote Sensing of the Earth." NASA Technical Memorandumn 81837, Langley Research Center; 1980.

[6] Lawrence, R. W.; Bailey, M. C.; Harrington, R. F.; Hearn, C. P. and Wells, J.: "Design and Development of a Multibeam 1.4 GHz Pushbroom Microwave Radiometer." NASA Technical Memorandumn 89005, Langley Research Center; 1986.

[7] Otoshi, T. Y. "The Effect of Mismatched Components on Microwave Noise-Temperature Calibrations." *IEEE Transactions on Microwave Theory and Techniques*, Vol MTT-16, No 9, pp 675-686, January 1968.

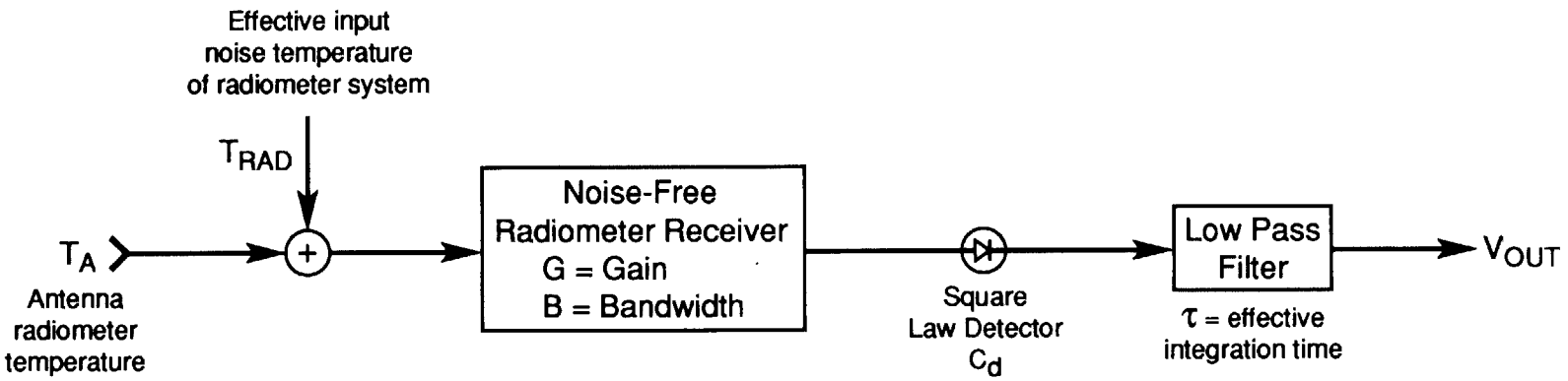

Figure 1. Total power radiometer system configuration.

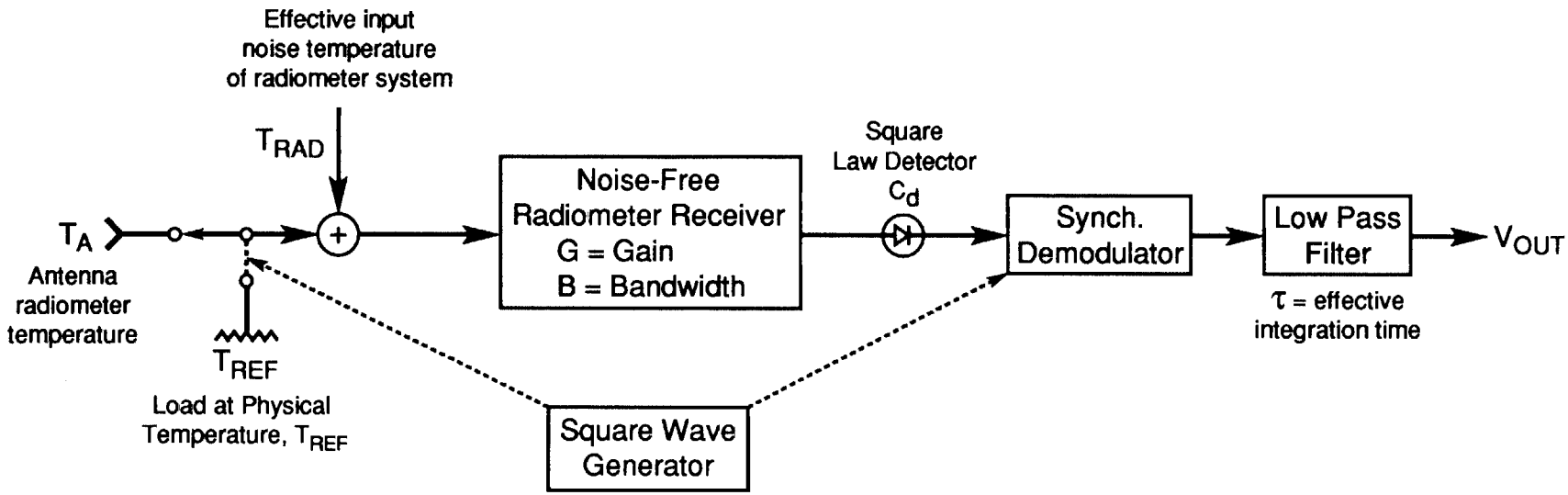

Figure 2. Unbalanced Dicke radiometer system configuration.

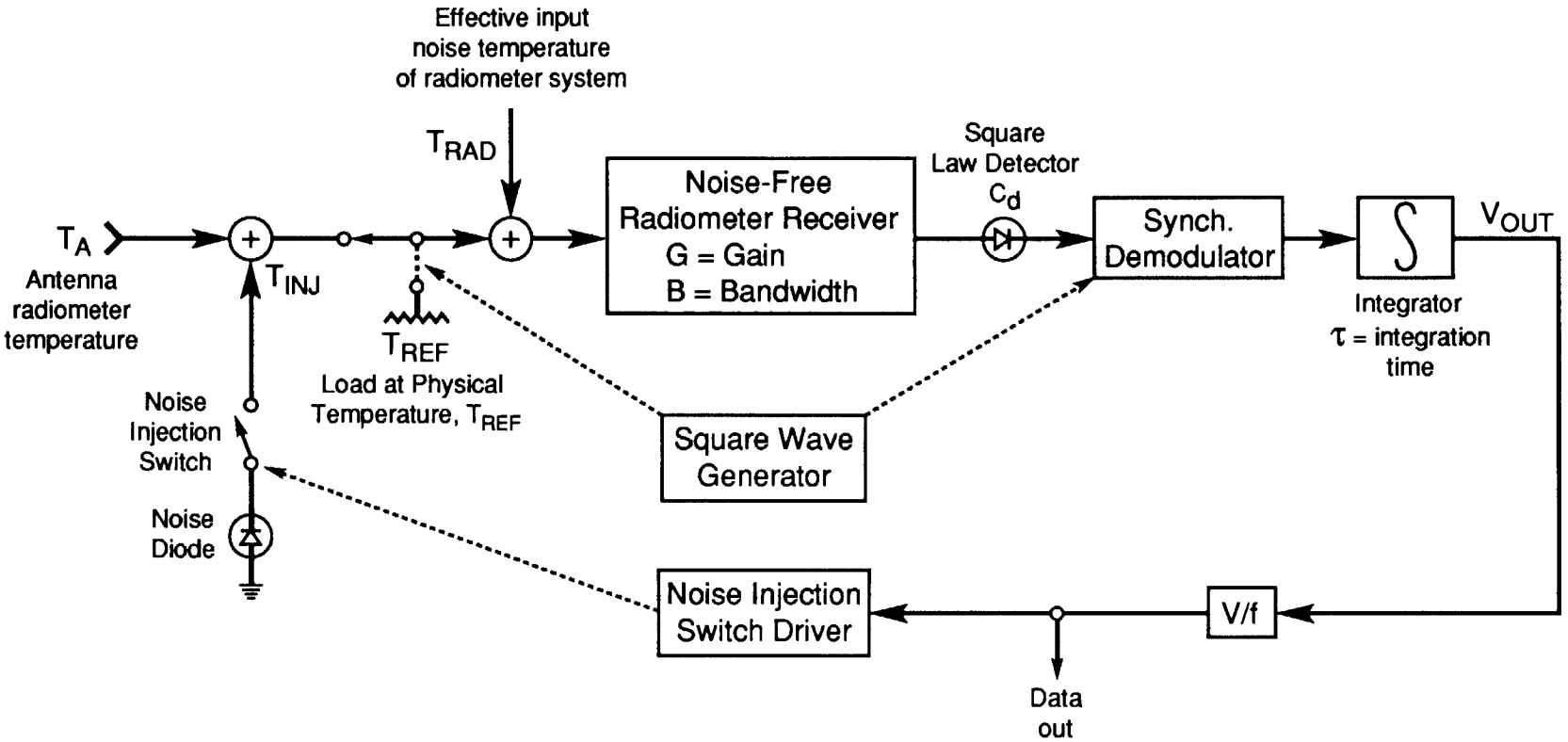

Figure 3. Balanced Dicke radiometer system configuration.

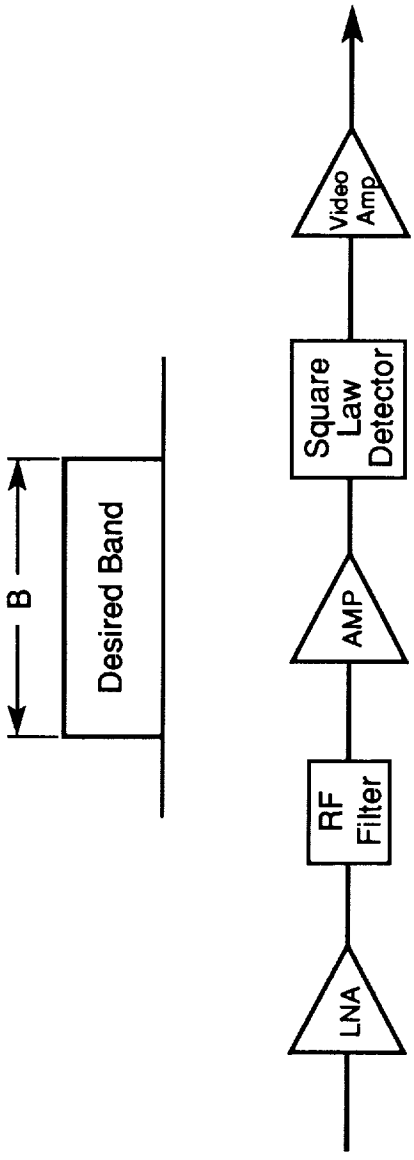

Figure 4. Direct detection receiver.

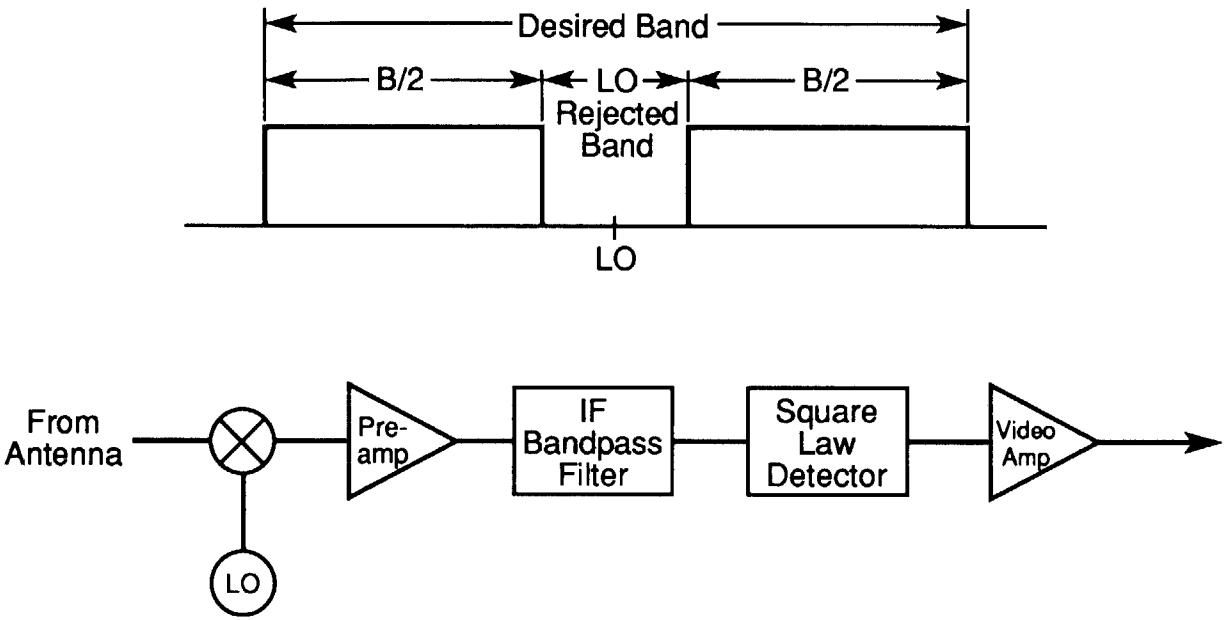

Figure 5. Double sideband homodyne receiver.

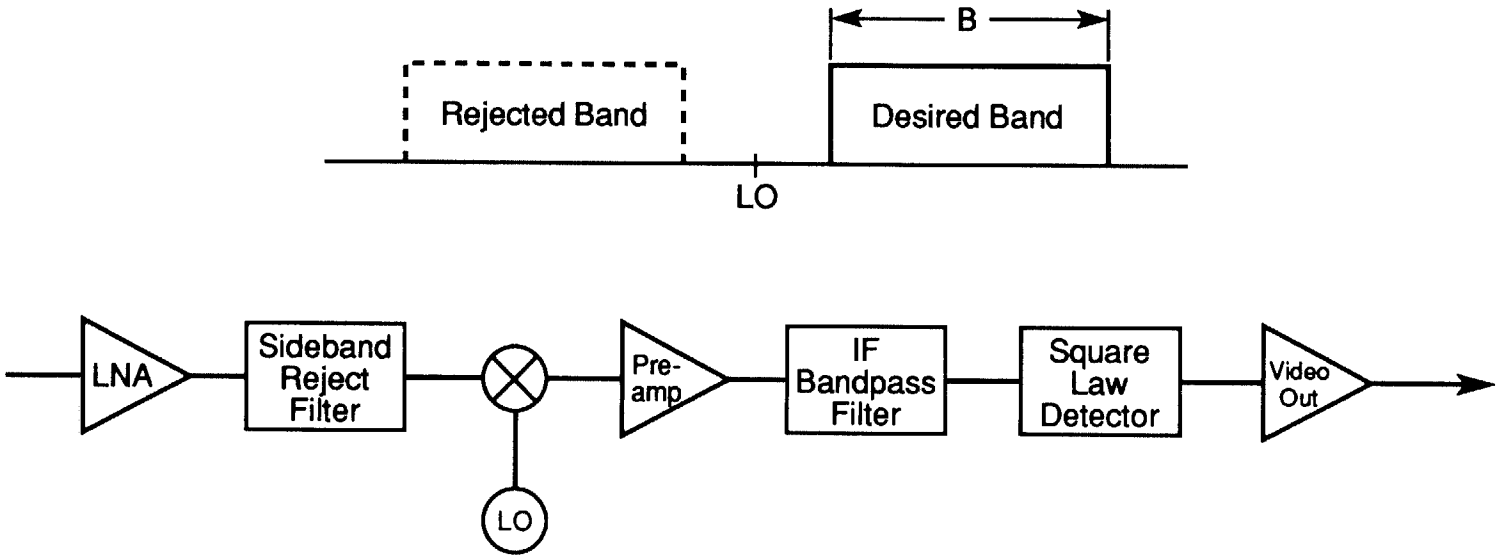

Figure 6. Single sideband heterodyne receiver.

REPORT DOCUMENTATION PAGE

Form Approved
OMB No. 0704-0188

1. AGENCY USE ONLY *(Leave blank)*	2. REPORT DATE	3. REPORT TYPE AND DATES COVERED
	April 1994	Contractor Report

4. TITLE AND SUBTITLE
Conceptual Radiometer Design Studies for Earth Observations From Low Earth Orbit

5. FUNDING NUMBERS
C NAS1-18584
TA 97
WU 233-01-03-22

6. AUTHOR(S)
Richard F. Harrington

7. PERFORMING ORGANIZATION NAME(S) AND ADDRESS(ES)
Old Dominion University Research Foundation
P.O. Box 6369
Norfolk, VA 23508-0369

8. PERFORMING ORGANIZATION REPORT NUMBER

9. SPONSORING/MONITORING AGENCY NAME(S) AND ADDRESS(ES)
National Aeronautics and Space Administration
Langley Research Center
Hampton, VA 23681-0001

10. SPONSORING/MONITORING AGENCY REPORT NUMBER
NASA CR-4588

11. SUPPLEMENTARY NOTES
Langley Technical Monitor: Lyle C. Schroeder
Final Report

12a. DISTRIBUTION/AVAILABILITY STATEMENT
Unclassified-Unlimited

Subject Category 43

12b. DISTRIBUTION CODE

13. ABSTRACT *(Maximum 200 words)*

A conceptual radiometer design study was performed to determine the optimum design approach for spaceborne radiometers in low Earth orbit. Radiometric system configurations which included total power radiometers, unbalanced Dicke radiometers, and balanced Dicke, or as known as noise injection, radiometers were studied. Radiometer receiver configurations which were analyzed included the direct detection radiometer receiver, the double sideband homodyne radiometer receiver, and the single sideband heterodyne radiometer receiver. Radiometer system performance was also studied. This included radiometric sensitivity analysis of the three different radiometer system configurations studied. Both external and internal calibration techniques were analyzed. An accuracy analysis with and without mismatch losses was performed. It was determined that the balanced Dicke radiometer system configuration with direct detection receivers and external calibrations was optimum where frequent calibration such as once per minute were not feasible.

14. SUBJECT TERMS	15. NUMBER OF PAGES
microwave radiometry, microwave receivers, radiometric sensitivity, mismatch errors	48
	16. PRICE CODE A03

17. SECURITY CLASSIFICATION OF REPORT	18. SECURITY CLASSIFICATION OF THIS PAGE	19. SECURITY CLASSIFICATION OF ABSTRACT	20. LIMITATION OF ABSTRACT
Unclassified	Unclassified		